ORNL/TM-2016/191
Revision: 0

Input Correlations for Irradiation Creep of FeCrAl and SiC Based on In-Pile Halden Test Results

Fuel Cycle Research & Development Advanced Fuels Campaign

K. A. Terrani
T. M. Karlsen
Y. Yamamoto

Prepared for
U. S. Department of Energy
Office of Nuclear Energy

May 2016
M2FT-16OR020201071

ORNL/TM-2016/191
Revision 0

Input Correlations for Irradiation Creep of FeCrAl and SiC Based on In-Pile Halden Test Results

K. A. Terrani
T. M. Karlsen
Y. Yamamoto

May 2016

Prepared by
OAK RIDGE NATIONAL LABORATORY
Oak Ridge, TN 37831-6283
managed by
UT-BATTELLE, LLC
for the
US DEPARTMENT OF ENERGY
under contract DE-AC05-00OR22725

INTENTIONALLY BLANK

ABSTRACT

Swelling and creep behavior of wrought FeCrAl alloys and CVD-SiC, two candidate accident tolerant fuel cladding materials, are being examined using in-pile tests at the Halden reactor. The outcome of these tests are material property correlations that are inputs into fuel performance analysis tools. The results are discussed and compared with what is available in literature from irradiation experiments in other reactors or out-of-pile tests. Specific recommendation on what correlations should be used for swelling, thermal, and irradiation creep for each material are provided in this document.

INTENTIONALLY BLANK

CONTENTS

Page

INTENTIONALLY BLANK

LIST OF FIGURES

Figure **Page**

INTENTIONALLY BLANK

LIST OF TABLES

Table **Page**

INTENTIONALLY BLANK

Input Correlations for Irradiation Creep of FeCrAl and SiC Based on In-Pile Halden Test Results

1. INTRODUCTION

In order to enhance safety margins during light water reactor (LWR) severe accidents an effort is underway to evaluate candidate accident tolerant cladding materials with the ultimate goal of replacing Zr-based alloy cladding in the core. SiC fiber reinforced SiC matrix (SiC/SiC) composites along with alumina forming ferritic alloys (FeCrAl) exhibit exceptional oxidation resistance in high-temperature steam environments [1]–[3] and therefore are two of the leading candidates to replace Zr-based alloys. Aside from their severe accident performance that has been carried out recently in a preliminary fashion [4]–[6], many other basic operational performance characteristics need to be evaluated to guide informed development and deployment strategies for these advanced cladding materials. Basic neutronic analyses to date have been carried out that require thin FeCrAl cladding (~350μm instead of ~600μm for Zr alloys) for sustainable fuel cycles [7]. For SiC/SiC cladding, neutronic penalty at the current cladding thickness does not prove limiting, however, behavior from a thermo-mechanical perspective needs to be better understood [8], [9].

In order to carry out informed thermo-mechanical analysis of either the thin metal cladding or the ceramic composite, a large set of materials properties data are necessary. Prominent amongst these are the thermal and irradiation creep rates for these materials. This is particularly important for LWR cladding since it consists of a thin tube housing a relatively large ceramic pellet. The cladding needs to exhibit a certain amount of creep so that the stresses that build up in the tube structure may be alleviated. The primary source of these stresses are the ones due to pellet-cladding mechanical interaction.

Defects that accumulate under irradiation may result in a number of macroscopic dimensional changes. These include swelling, growth, and irradiation creep among other effects [3]. Irradiation swelling strictly refers to an isotropic volume increase in an unstressed material caused by the formation of irradiation-induce defects, resulting from the agglomeration of point defects and gas atoms inside the material. Growth is defined as anisotropic deformation of the material where the volume is strictly conserved. Creep in general is defined as time-dependent deformation of materials at constant volume under deviatoric stress below the yield stress as a result of thermally activated processes. The strict definition of irradiation creep strain is the difference in plastic strain in addition ot thermal creep between two specimens under the same irradiation condition with and without stress loading. The role of irradiation is to induce or accelerate the creep deformation through various mechanisms [10]. Irradiation creep is usually athermal and has a first order dependence on dose and stress.

Zr-based alloys undergo irradiation growth as well as thermal and irradiation creep [11], [12] while swelling in these alloys is very negligible in the absence of noble gases. Crystalline and high purity SiC undergoes substantial swelling that saturates at a relatively low dose (<1dpa) within the temperature range applicable for LWR cores [13]–[15]. Although thermal creep is negligible at T<1400°C [16] for SiC, an irradiation creep rate that decreases as swelling saturates has been previously reported for this material [17]–[19]. Swelling behavior of ferritic steels has received ample attention in the past and is known to be negligible in the dose range applicable to LWR fuel cladding [20]. Thermal creep is a strong function of alloy composition and microstructure and in case of FeCrAl alloys it has only received limited attention at high temperatures (≥500°C) [21]. Finally, irradiation creep has received some attention with rough estimates available for bcc metals in the literature [20], [22], [23].

2. EXPERIMENT DESCRIPTION

The focus of this experiment is in-pile creep testing of wrought FeCrAl alloys and chemical vapor deposited (CVD) SiC specimens to produce reliable in-pile data on creep compliance coefficient of these materials as a function of dose at a given temperature. Only a limited temperature is probed that is directly applicable to the temperature of LWR fuel cladding under normal operating conditions. For FeCrAl alloys the test temperature was fixed at 350°C. In case of SiC, in order to exaggerate the swelling that is inversely proportional to the temperature, the test temperature was kept constant at 300°C.

The creep tests take advantage of in-pile instrumentation and control systems native to the Halden facility to collect accurate in-pile data with reliable environmental controls. Detailed description of this test rig is provided elsewhere [24], but briefly, it utilizes adjustable mixture gas flow in annular regions of the capsule, coupled with multiple thermocouples in each capsule for precise temperature control along the length of the specimen. The stress on the creep specimens is controlled by direct gas pressure control inside a bellow attached to the creep specimen that is gripped at the other end. The creep strain is measured directly using a calibrated linear variable differential transformer (LVDT) that is in contact with the end of the specimen. Figure 1 shows a schematic of the in-pile creep test rig.

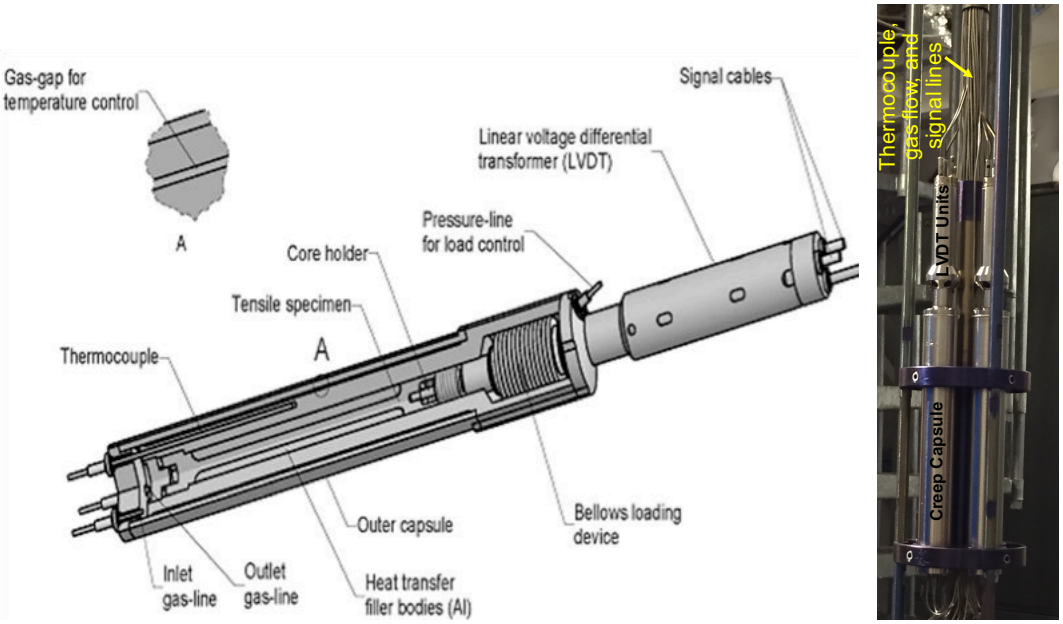

Fig. 1. Left: Schematic of instrumented in-pile creep test rig from ref. [24]**, Right: four creep capsules utilized in this test on top of IFA-744 test rig prior to insertion into the Halden reactor.**

Throughout the experiment the total deformation strain of the material under stress in the in-pile conditions is measured. This quantity is the sum of strains due to elastic strain, thermal expansion, linear swelling, thermal creep, and irradiation creep, Eq. (1). At a constant load and temperature, two of the three parameters in the right hand side of Eq. (1) need to be known to distinguish the various terms.

$$\varepsilon_{total} = \varepsilon_{elastic} + \varepsilon_{CTE} + \varepsilon_{swelling} + \varepsilon_{thermal\ creep} + \varepsilon_{irradiation\ creep} \quad (1)$$

2.1 TEST MATERIALS

Two SiC specimens machined from high-purity chemical vapor deposited (CVD) SiC were examined in this study. The CVD variant, of purity >99.999%, was purchased from Dow Chemical Co. (Marlborough, MA). The specimens were machined so that the uniaxial loading direction was perpendicular to CVD growth direction. The specimens were not annealed after the CVD processing step. 13 fiducial marks were etched on the gauge section of each specimen (Figure 2) and their locations were recorded accurately to provide the basis for verification of in-pile strain data during the post irradiation examination (PIE).

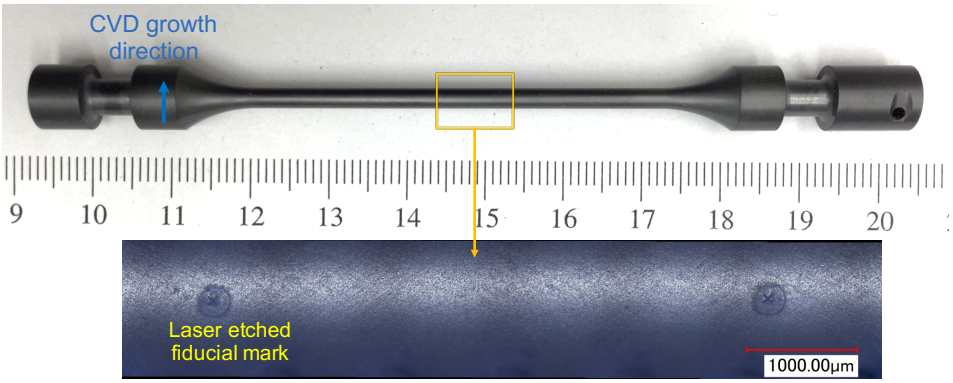

Fig. 2. CVD-SiC tensile bars used for in-pile swelling/creep tests.

Also, three FeCrAl specimens from two distinct alloys were examined. The FeCrAl alloys were produced at ORNL and they were designated as C35M2 and C35MN5. The composition of the alloys is provided in Table 1. C35M2 alloy was hot-forged at 650°C with 75% area reduction (36mm diameter round bar to 16 mm square bar), followed by annealing at 650°C for 1h. Microstructure of this alloy consisted of deformed (elongated) grains. Note that the final annealing was applied to stabilize fine sub-grain (SG) structure, with ~1-5 µm size inside of the elongated grains. C35MN5 alloy was hot-extruded at 800°C with 88% area reduction (2.9" diameter to 1.0" diameter), followed by annealing at 800°C for 1h. Microstructure consists of highly deformed (elongated) grains, which shows a dense dispersion of Nb-rich second-phase precipitates (Figure 3). Extensive detail on processing and properties of these alloys is provided elsewhere [25]. The exact drawings for the FeCrAl and SiC tensile specimens are provided at the end of this document as appendices.

Table 1. Analyzed chemistry of the ORNL ATF FeCrAl alloys studied

Heat	Analyzed composition [wt%]										
	Fe	Cr	Al	Mo	Si	Nb	Y	C	N	O	S
C35M2	79.67	13.06	5.15	1.97	0.12	-	0.010	0.004	0.0021	0.0017	0.0015
C35MN5	78.68	13.02	5.08	1.99	0.21	0.97	0.032	0.003	0.0013	0.0028	0.0003

2.2 TEST CONDITIONS

The specimens are tested in the stress-free and stressed conditions to determine the swelling-induced deformation only, as well as the swelling and creep-induced deformations combined (as noted in Eq. (1)). Note that a small stress (~5MPa) is applied under the nominally stress-free conditions to ensure the

specimen remain in good contact with the LVDT. The test conditions are described in Table 2. Note that the stress on the SiC specimen is maintained at 100 MPa. However, the stress level on the FeCrAl specimens is varied over time to determine the creep rate as a function of stress. Also, since thermal creep may not be ignored for FeCrAl alloys, a separate series of out-of-pile creep tests at the exact temperature and stress levels are being carried out at ORNL. In this manner the magnitude of thermal creep could be determined separately. The starting stress for FeCrAl alloys was set at a high value of 325 MPa that is just below the yield stress of these alloys at 350°C (Figure 4). This stress is representative of a value that is expected to develop in the thin cladding under fuel pin operation, particularly upon fuel-pellet contact.

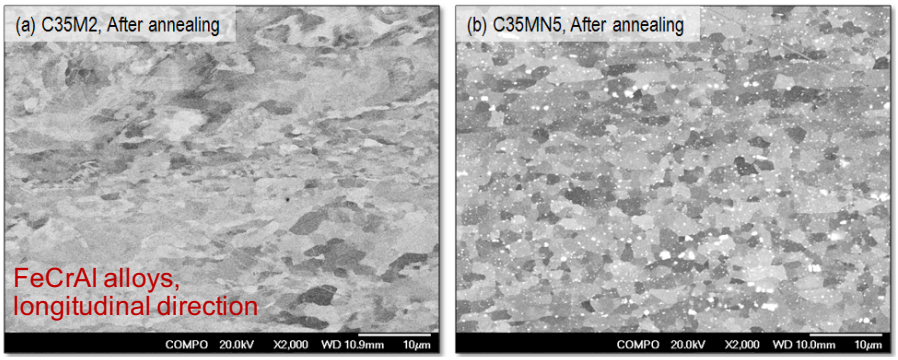

Fig. 3. Backscattered electron micrographs of a) C35M2 and b) C35MN5 alloys.

Table 2. In-pile creep test parameters.

Specimen	Temperature [°C]	Stress [MPa]					
C35MN5C-1	350	325	250	200	100	350	325
C35M2-1	350	325	250	200	100	350	325
C35M2-2	350	0					
SiC-1	300	100					
SiC-2	300	0					

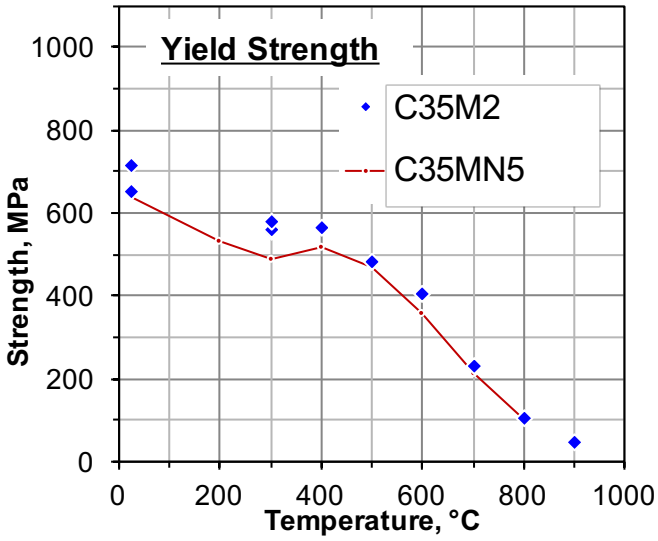

Fig. 4. Yield strength as a function of temperature for the FeCrAl alloys examined in this study.

2.3 DPA RATE DURING IN-PILE TEST

Since irradiation creep is directly proportional to the damage induced in the material as a result of neutron fluence, it is essential to perform accurate calculation of damage production rates in these materials. This is particularly important when the results from the tests in a research reactor are to be compared with results from other research reactors or applied to predict the material behavior in commercial reactors. In order to perform dpa calculations, flux spectrum (flux per unit energy, $\varphi_g[E]$) that is experienced by the specimen is necessary. The total flux, ϕ, is the sum of the flux in each energy group. Flux spectra for HFIR (in the flux trap target (FTT) peripheral target position (PTP) at the midplane location) and Halden (IFA-744 rig at the location of creep capsules), are shown in Figure 5 and 6, where the former is normalized per unit lethargy. The total flux for the HFIR and Halden positions is ~4.46×10^{15} and ~1.20×10^{14} n/cm^2-s, respectively. However, the spectra differ significantly, as shown in Fig. 2 where fast flux is roughly two orders of magnitude larger in HFIR.

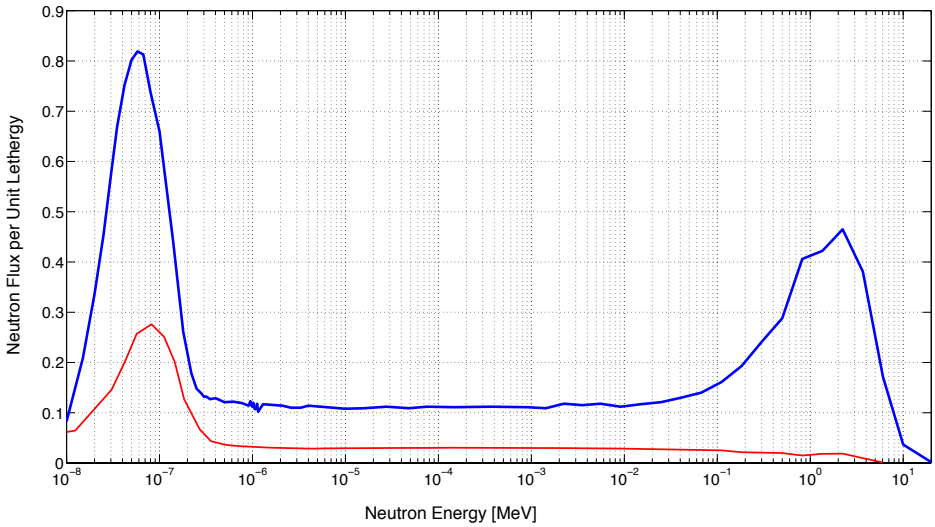

Fig. 5. Neutron flux spectra per unit lethargy in Halden IFA-744 test rig (red) and HFIR PTP position (blue).

The goal is to calculate the dpa (displacement per atom) rate in the materials of interest. The dpa rate can be calculated as:

$$\dot{d} = \int \varphi_g(E)\sigma_d(E)dE \qquad (2)$$

where σ_d is the displacement cross section. The displacement cross section for SiC [26] and pure Fe [27] are shown in Fig. 7. Also shown is the dpa cross section for Fe-13Cr-5Al alloy, calculated simply by weighing in the mole fraction of Cr and Al in the alloy and accounting for their dpa cross section from the same reference as for pure Fe. Note that the dpa cross section for the alloy is binned differently than that of pure Fe (larger energy bins) and appears smoother than the Fe dpa cross section. The dpa rate for these materials in Halden's IFA 744 and HFIR's FTT-PTP are tabulated in Table 3. These results were also compared with the output from the SPECTER code [28] and they were in good agreement. The reactor power and fast neutron flux (E >1 MeV) in the vicinity of creep capsules as a function of time are plotted in Figure 8.

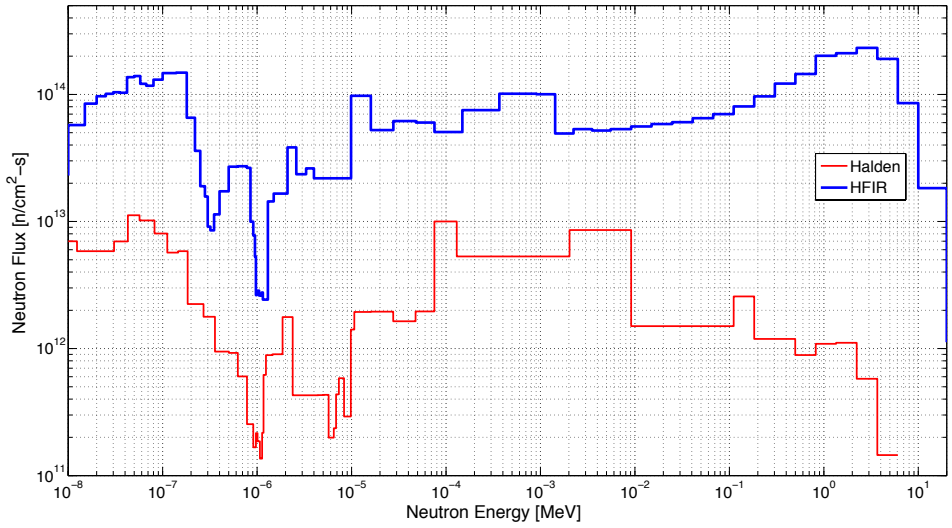

Fig 6. Neutron flux spectra in Halden IFA-744 test rig and HFIR PTP position.

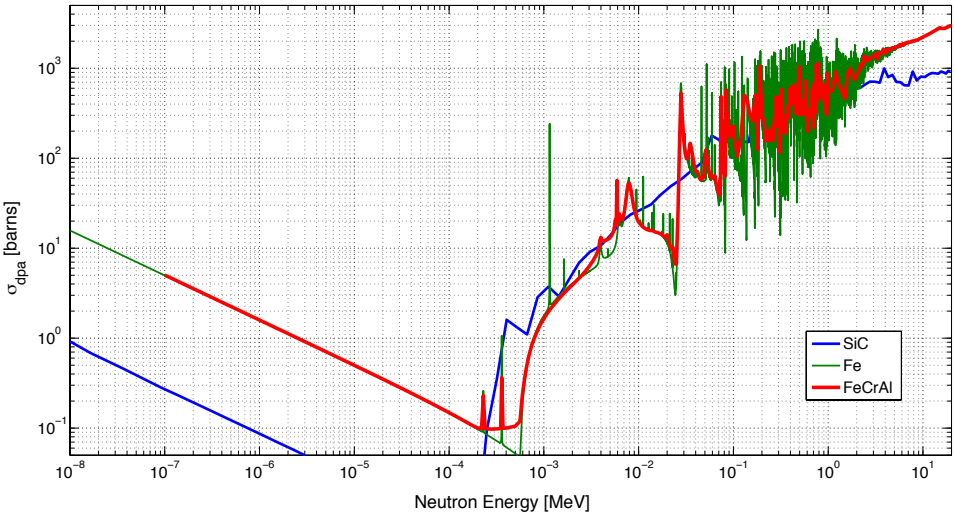

Fig. 7. dpa cross sections in barns for SiC, Fe, and Fe-13Cr-5Al as a function of neutron energy in MeV. The cross sections for Fe and FeCrAl are based on the NRT approach.

Table 3. dpa rate in SiC and Fe in HFIR and Halden calculated using various dpa cross sections

	dpa/s	dpa/HFIR[1] Cycle	dpa/month	dpa/1000h	dpa/EFPY
CVD-SiC - dpa cross section from [12]					
Halden IFA 744	3.59E-09		0.009	0.013	0.113
HFIR FTT-PTP	7.59E-07	1.57	1.97	2.73	23.84
Pure Fe – NRT[2]					
Halden IFA 744	4.94E-09		0.013	0.018	0.155
HFIR FTT-PTP	9.53E-07	1.98	2.47	3.43	29.94
FeCrAl – NRT[2]					
Halden IFA 744	4.63E-09		0.012	0.017	0.145
HFIR FTT-PTP	1.05E-06	2.18	2.72	3.78	32.99

[1]HFIR cycle of 24 days is assumed.
[2]NRT → Norget-Robinson-Torrens [29].

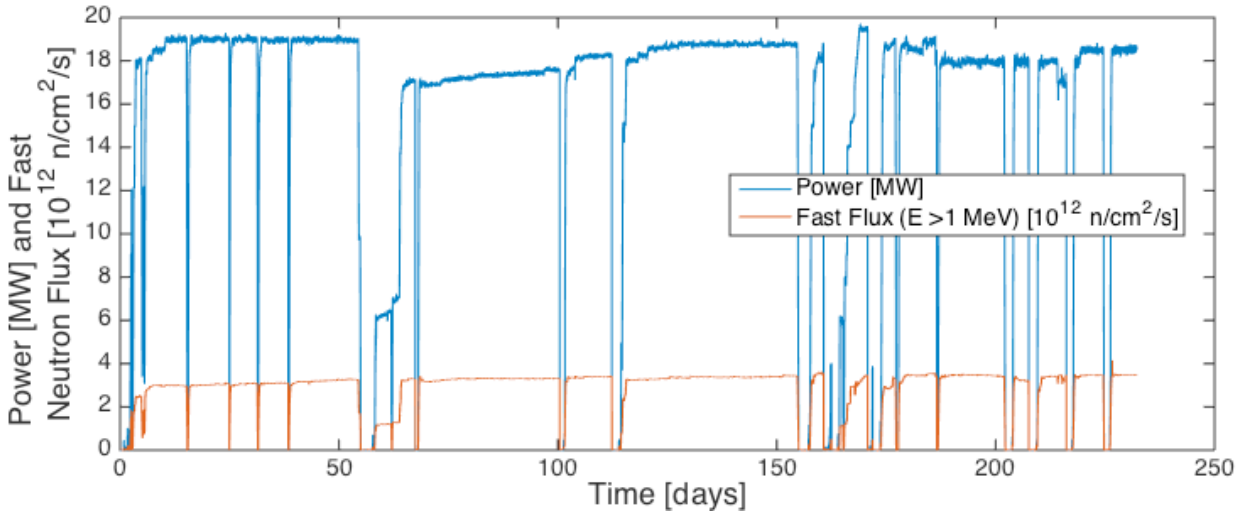

Fig. 8. Reactor power and fast neutron flux as a function of time.

3. RESULTS

3.1 IN-PILE CREEP OF SiC

Figure 9 shows the results from in-pile measurement of displacement in SiC specimens along with the applied stress and continuous measurement of temperature. The figure plots the high-quality displacement dataset as function of dose. A clear and significant departure in strain rate between the two samples is observed upon application of 100 MPa of stress on the creep specimen. Figure 10 compares the swelling and creep strain experienced by these specimens with discrete swelling strain data from specimens irradiated in HFIR where the two appear to be in good agreement.

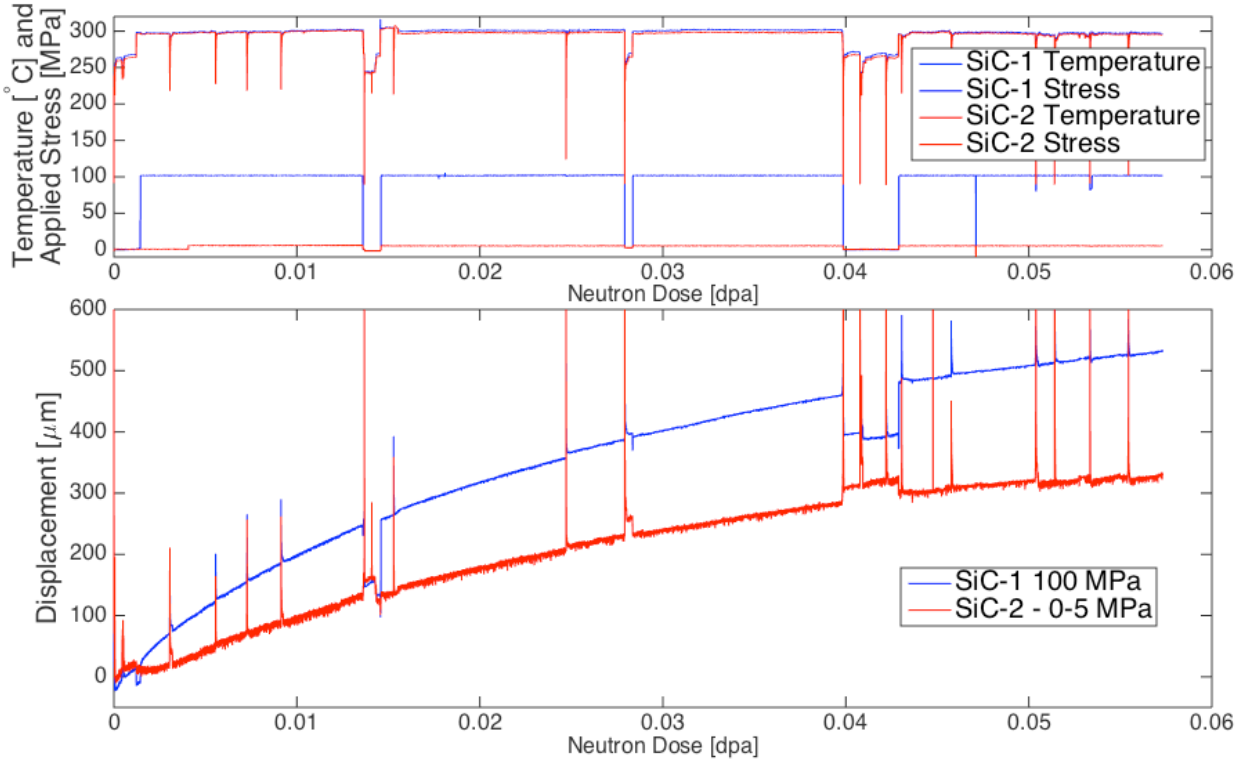

Fig. 9. Temperature, stress, and displacement as a function of neutron dose applied and experienced by SiC specimens.

As described in Eq. (3), The difference in the instantaneous strain rate of stressed and stress-free SiC specimens, normalized per unit stress, is the instantaneous irradiation creep compliance (B) of SiC.

$$B = \frac{\dot{\varepsilon}_{stressed} - \dot{\varepsilon}_{unstressed}}{\sigma \emptyset} \qquad (3)$$

The irradiation creep compliance is plotted as function of neutron dose in Fig. 11 and it appears to follow logarithmic creep behavior within this dose range. It is also compared with irradiation creep compliance data from bend stress relaxation (BSR) tests in HFIR [17], [18]. The creep compliance measured here appears significantly larger than the prior HFIR results. The reason for this difference, if indeed true, is not yet fully understood and may be attributed to any of the following items:

- Loading mode: uniaxial tension vs. bend stress relaxation
- Annealing: BSR specimens were annealed at 1900°C prior to irradiation

- Dose rate: factor ~200 higher in HFIR irradiation tests
- Neutron spectrum: much softer in Halden tests

Note that, as obvious from Eq. (3), the irradiation creep compliance can be defined only when the irradiation creep rate is proportional to the stress magnitude. The stress exponent was not confirmed to be unity in the present Halden experiment (in contrast to what was done previously for the HFIR BSR tests [17]). Alas, these large difference in irradiation creep rate needs to be verified during the PIE by measurement of distance between the fiducial marks etched on the gauge section of SiC tensile bars (Figure 2). Until these results are verified and explained, it is recommended that the fuel modelers continue to use the correlation provided in refs. [17], [18].

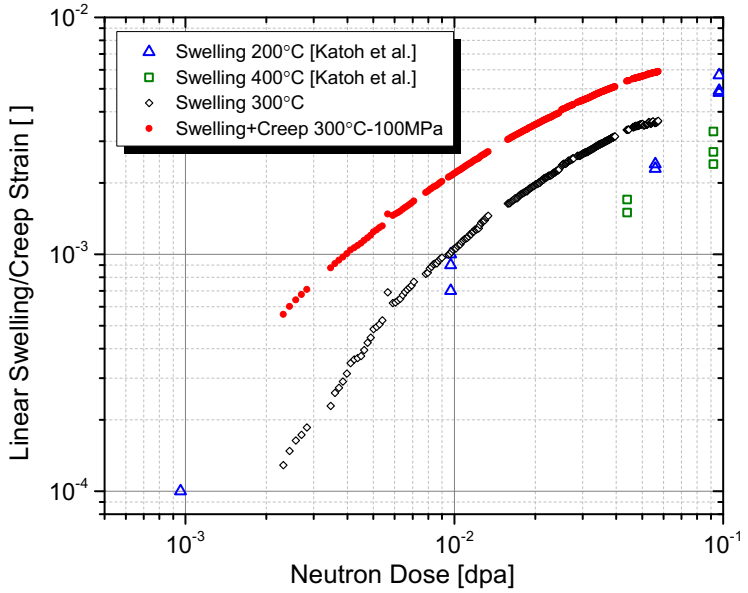

Fig. 10. Swelling and creep strain of SiC samples in the Halden experiment compared with swelling data from HFIR specimens from ref [15]**.**

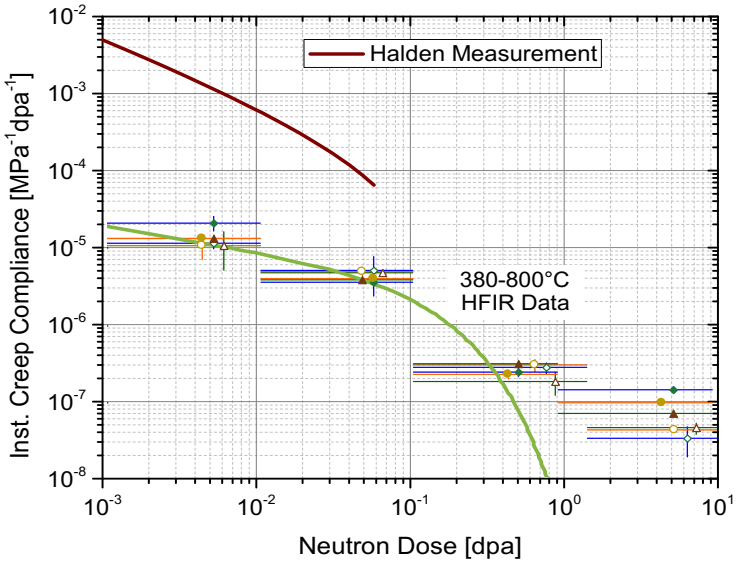

Fig. 11. Instantaneous irradiation creep compliance of SiC measured in Halden at 300°C and compared with results from HFIR tests from refs. [17], [18]**.**

3.2 OUT-OF-PILE CREEP OF FeCrAl

Out-of-pile creep tests are being performed on unirradiated FeCrAl specimens from the same exact batch of materials that are undergoing testing at Halden in irradiation creep capsules. The purpose of the out-of-pile tests is to separately determine the thermal creep rate in these alloys and to be able to distinguish all the distinct terms on the right-hand-side of Eq. (1). The tests were conducted at 350°C in an inert atmosphere on the C35M2 and C35MN5C alloys. The out-of-pile creep strain as a function of time is plotted in Figure 12. The thermal creep rate measured here for these alloys appears to be significantly (2-3 orders of magnitude) larger than the correlation reported in ref. [21]. However the correlation in ref. [21], written out in Eq. (4), is based on a limited set of high temperature data in that study alongside prior literature data at lower temperatures as shown in Figure 13.

$$\frac{\dot{\varepsilon}}{\sigma^{5.5}} = 5.96\times10^{-27}\exp\left(\frac{-392\ [\frac{kJ}{mole}]}{RT}\right) \qquad (4)$$

The creep rate and stress are in s^{-1} and Pa, respectively. As noted in the figure, if the correlation is limited to data for T<600°C, a much lower activation energy is attained. The fit to low temperature data is provided in Eq. (5).

$$\frac{\dot{\varepsilon}}{\sigma^{5.5}} = 1.04\times10^{-32}\exp\left(\frac{-247\ [\frac{kJ}{mole}]}{RT}\right) \qquad (5)$$

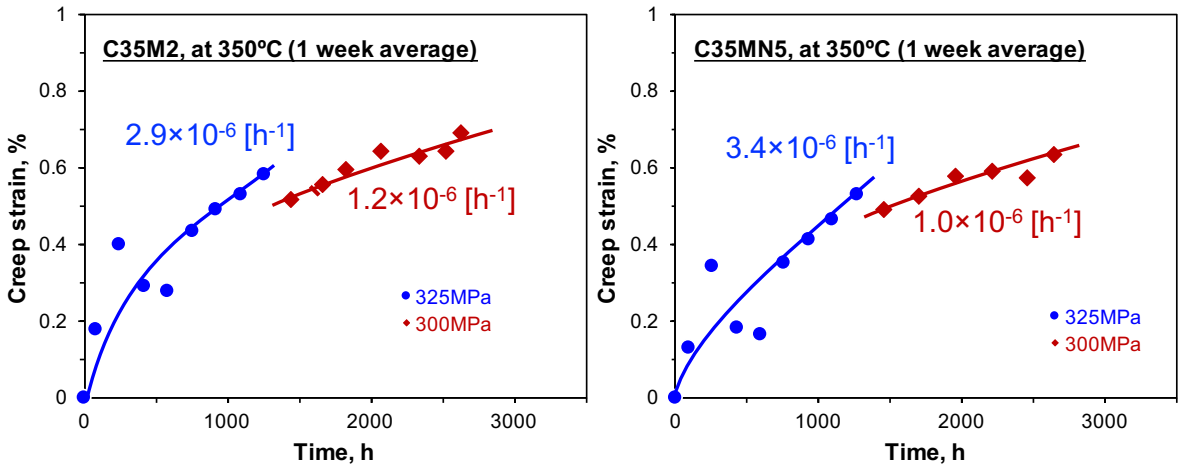

Fig. 12. Out-of-pile creep strain as a function of time on FeCrAl alloys.

Figure 14 provides a broad comparison between the out-of-pile creep data from Figure 12, Eqs. (4, 5), and also Zircaloy creep data from ref. [30]. As shown in the figure, experimental data agree relatively well with the low temperature correlation in Eq. (5) while Eq. (4) greatly underpredicts these data. In any case, the low temperature thermal creep correlation in Eq. (5) appears to be roughly two orders of magnitude smaller than what is experienced by Zr-based alloys.

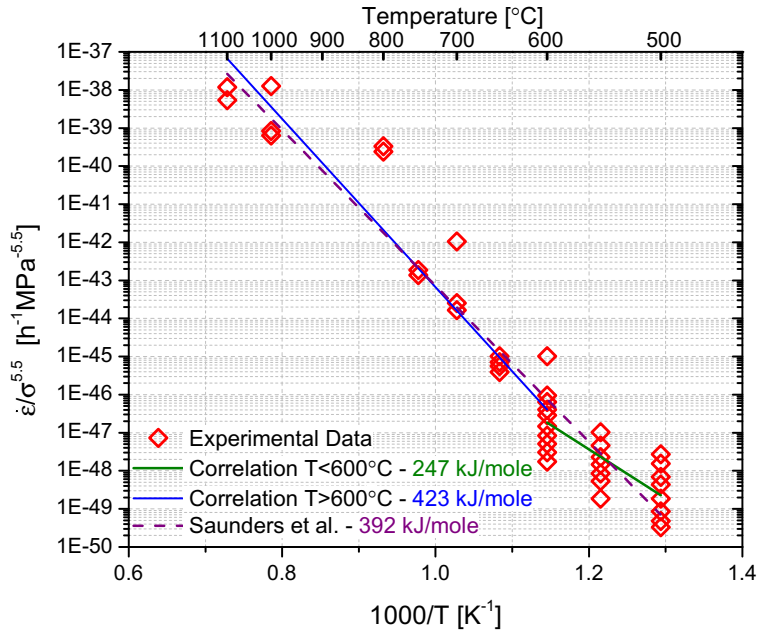

Fig. 13. Out-of-pile creep strain as a function of time on FeCrAl alloys.

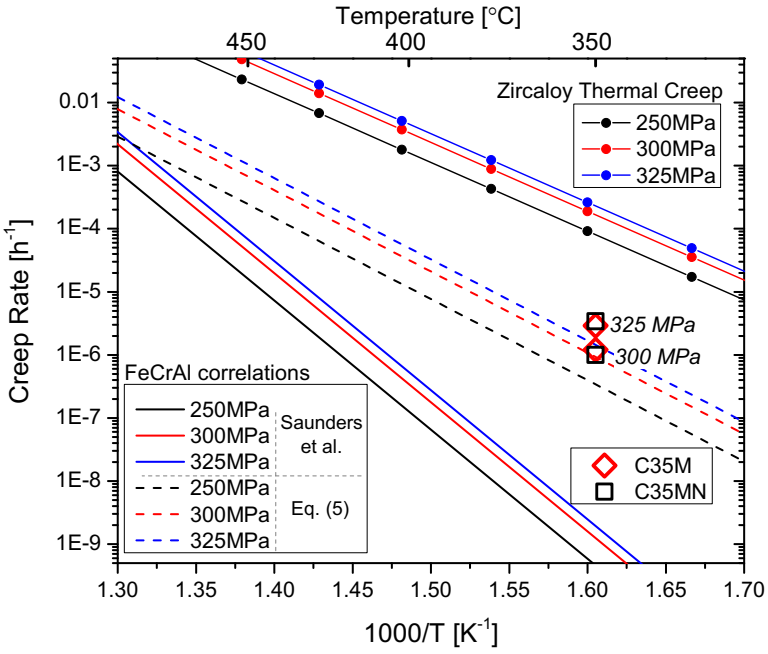

Fig. 14. Comparison between creep strain rate as a function of temperature between FeCrAl experimental data in Figure 12, correlations in Eqs. (4, 5), and Zircaloy correlations from ref. [30].

3.3 IN-PILE CREEP OF FeCrAl

Figure 9 shows the results from in-pile measurement of displacement in FeCrAl specimens along with the exact levels of applied stress and continuous measurement of temperature. The figure plots the displacement dataset as function of dose while the creep rate as a function of time is also designated for

each portion of the strain data. A clear and significant departure in strain rate between the stressed and stress-free C35M samples is observed upon application of 325 MPa of stress on one of the specimens. In fact, within the dose range experienced by the C35M alloy, no swelling strain can be discerned in the stress-free sample. This is consistent with what is expected in ferritic alloys within this dose regime and up to at least a few tens of dpa (beyond what is expected within their lifetime as LWR fuel cladding [20]. The displacement data for C35MN specimen were excluded due to faulty instrumentation during the in-pile tests. Analysis of the creep strain for this specimen will be carried out during the PIE.

A comparison between the in-pile and out-of-pile creep strain rate experienced by these specimens shows that very similar values are attained in both tests. This is indicative of the small relative magnitude of irradiation creep when compared with the thermal creep rate in this alloy. This is consistent with the estimates in the literature where irradiation creep in bcc metals is on the order of $0.5–5\times10^{-6}$ $MPa^{-1}dpa^{-1}$ [20], [22]. Within this range the displacement due to irradiation creep is <6μm; essentially undetectable in these tests. This is the case since the dose rate is very low in the Halden tests and the effort is currently focusing on introduction of booster rods to increase the fast flux in the periphery of the creep capsules.

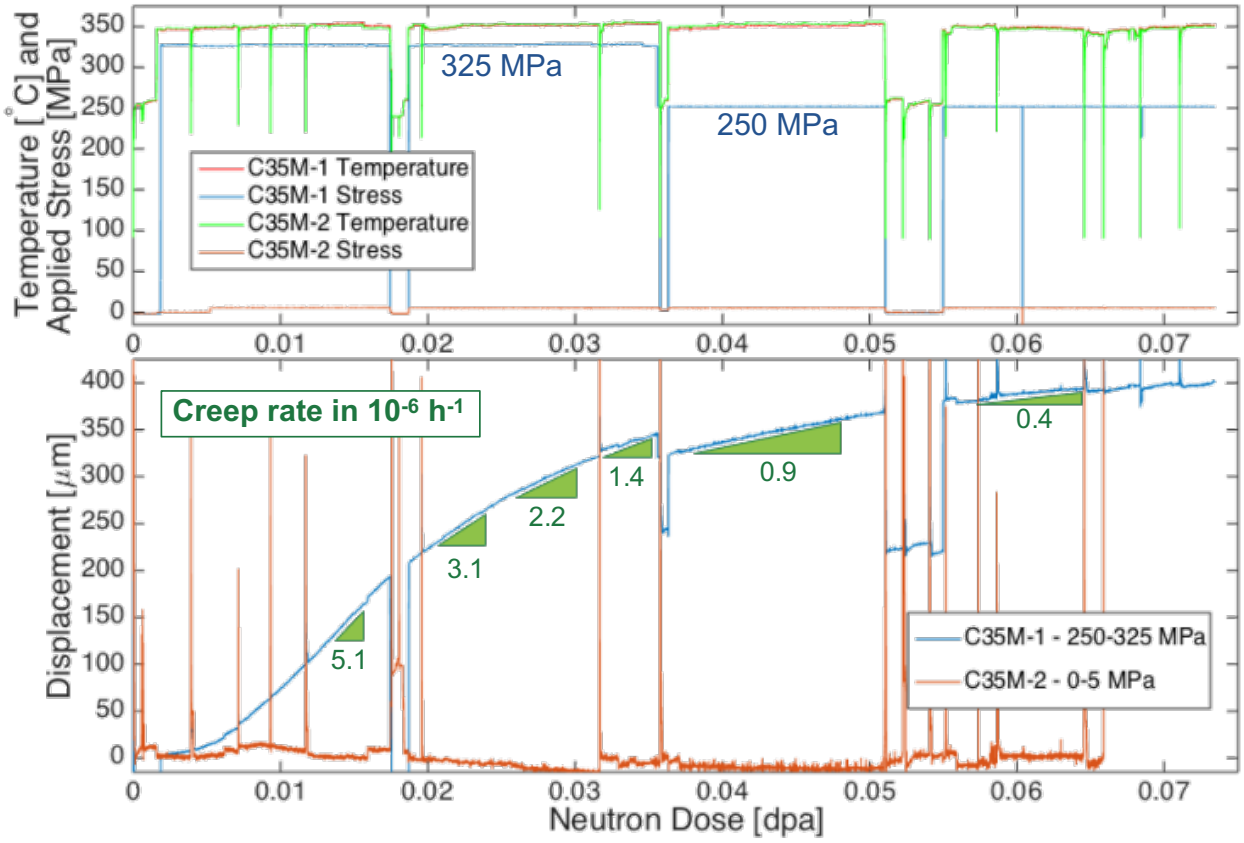

Fig. 15. Temperature, stress, and displacement as a function of neutron dose applied and experienced by FeCrAl specimens.

4. RECOMMENDATIONS ON SWELLING AND CREEP CORRELATION FOR FUEL PERFORMANCE MODELERS

The following are recommended to be used by fuel performance modelers tasked with analysis of FeCrAl- and SiC-based ATF cladding concepts. It should be noted that given the limited availability of experimental data, the modeling should be executed using a parametric approach. In this manner, the models better serve development activities while being able to prescribe design targets for material developers working on ATF related fuels and materials.

4.1 SiC CORRELATIONS

SiC swelling: the current data agree very well with prior observations in literature [13]–[15]. It is recommended that correlations provided in ref. [14] (Eqs. 3 and 4 in that reference) be utilized to predict swelling as a function of temperature and dose.

SiC thermal creep: a value of nil should be assigned to this parameter since it the mechanism is wholly absent at T<1400°C.

SiC irradiation creep: Although the results in this study point to an irradiation creep compliance much larger than previously reported, they need to be verified during the PIE tests and are not yet recommended to be used for fuel performance analysis. Modelers should continue to use correlations in ref. [17] (Eq. 6 in that reference).

4.2 FeCrAl CORRELATIONS

FeCrAl swelling: Due to the very low dose rates, no discernable swelling is observed in the FeCrAl alloys in this study. This is expected and consistent with numerous prior literature such as data in ref. [20]. It is recommended that parametric swelling rates of nil and 0.05%/dpa (applicable within the LWR dose regime of <20 dpa) are used for the analysis.

FeCrAl thermal creep: Given the limited availability of data it is recommended that Eq. (5) in this report is utilized for preliminary modeling analyses.

FeCrAl irradiation creep: The value recommended for irradiation creep compliance of wrought FeCrAl is $\sim 5\times10^{-6}$ $MPa^{-1}dpa^{-1}$. This estimate is higher than what is measured for ferritic/martensitic steels studied in ref. [20], however, given the larger ferrite grain without a high density of boundaries or precipitates it is warranted.

5. SUMMARY AND OUTLOOK

A set of in-pile creep tests is ongoing in the Halden reactor on two candidate accident tolerant fuel cladding material and constituents: wrought FeCrAl alloys and CVD-SiC. These tests are meant to provide essential material property information that is needed for an informed analysis of these fuel concepts under normal operating conditions. These tests provide detailed information regarding swelling, thermal creep, and irradiation creep rates of these materials. The results to date have been compared with the limited set of information available in literature that is form irradiation tests in other reactors or out-of-pile tests. Most of the results are in good agreement with prior literature, except for irradiation creep rate of SiC. To elucidate the difference between the HFIR and Halden test results continued testing and PIE is necessary. The tests describe in this progress report are ongoing and will continue for roughly 3 more months for SiC specimens and longer for FeCrAl alloys. The former are to be extracted for subsequent PIE after the completion of the next reactor cycle.

INTENTIONALLY BLANK

REFERENCES

[1] B. A. Pint, K. A. Terrani, M. P. Brady, T. Cheng, and J. R. Keiser, "High Temperature Oxidation of Fuel Cladding Candidate Materials in Steam-Hydrogen Environments," *J. Nucl. Mater.*, vol. 440, pp. 420–427, 2013.

[2] K. A. Terrani, B. A. Pint, C. M. Parish, C. M. Silva, L. L. Snead, and Y. Katoh, "Silicon Carbide Oxidation in Steam up to 2 MPa," *J. Am. Ceram. Soc.*, vol. 97, no. 8, pp. 2331–2352, 2014.

[3] B. A. Pint, K. A. Terrani, Y. Yamamoto, and L. L. Snead, "Material Selection for Accident Tolerant Fuel Cladding," *Metall. Mater. Trans. E*, 2014.

[4] L. J. Ott, K. R. Robb, and D. Wang, "Preliminary assessment of accident-tolerant fuels on LWR performance during normal operation and under DB and BDB accident conditions," *J. Nucl. Mater.*, vol. 448, pp. 520–533, 2014.

[5] K. R. Robb, "Analysis of the FeCrAl Accident Tolerant Fuel Concept Benefits During BWR Station Blackout Accidents," *Proceedings of the 16th International Topical Meeting on Nuclear Reactor Thermal Hydraulics (NURETH-16)*. Chicago, IL, USA, pp. 1183–1195, 2015.

[6] B. J. Merrill and S. M. Bragg-Sitton, "SiC Modifications to MELCOR for Severe Accident Analysis Applications," Idaho National Laboratory (INL), 2013.

[7] N. M. George, K. Terrani, J. Powers, A. Worrall, and I. Maldonado, "Neutronic analysis of candidate accident-tolerant cladding concepts in pressurized water reactors," *Ann. Nucl. Energy*, vol. 75, pp. 703–712, 2015.

[8] M. Ben-Belgacem, V. Richet, K. A. Terrani, Y. Katoh, and L. L. Snead, "Thermo-mechanical analysis of LWR SiC/SiC composite cladding," *J. Nucl. Mater.*, vol. 447, no. 1–3, pp. 125–142, 2014.

[9] Y. Lee and M. S. Kazimi, "A structural model for multi-layered ceramic cylinders and its application to silicon carbide cladding of light water reactor fuel," *J. Nucl. Mater.*, vol. 458, pp. 87–105, 2015.

[10] K. Ehrlich, "Irradiation creep and interrelation with swelling in austenitic stainless steels," *J. Nucl. Mater.*, vol. 100, no. 1, pp. 149–166, 1981.

[11] C. H. Woo, "Modeling irradiation growth of zirconium and its alloys," *Radiat. Eff. Defects Solids*, vol. 144, no. 1–4, pp. 145–169, 1998.

[12] R. A. Holt, "Microstructure dependence of irradiation creep and growth of zirconium alloys," *J. Nucl. Mater.*, vol. 90, no. 1–3, pp. 193–204, 1980.

[13] L. L. Snead, T. Nozawa, Y. Katoh, T. S. Byun, S. Kondo, and D. A. Petti, "Handbook of SiC properties for fuel performance modeling," *J. Nucl. Mater.*, vol. 371, no. 1–3, pp. 329–377, 2007.

[14] Y. Katoh, K. Ozawa, C. Shih, T. Nozawa, R. J. Shinavski, A. Hasegawa, and L. L. Snead, "Continuous SiC fiber, CVI SiC matrix composites for nuclear applications: Properties and irradiation effects," *J. Nucl. Mater.*, vol. 448, pp. 448–476, 2014.

[15] Y. Katoh, T. Nozawa, L. L. Snead, K. Ozawa, and H. Tanigawa, "Stability of SiC and its composites at high neutron fluence," *J. Nucl. Mater.*, vol. 417, no. 1–3, pp. 400–405, 2011.

[16] C. H. CARTER, R. F. DAVIS, and J. BENTLEY, "Kinetics and Mechanisms of High-Temperature Creep in Silicon Carbide: II, Chemically Vapor Deposited," *J. Am. Ceram. Soc.*, vol. 67, no. 11, pp. 732–740, 1984.

[17] Y. Katoh, L. L. Snead, C. M. Parish, and T. Hinoki, "Observation and possible mechanism of irradiation induced creep in ceramics," *J. Nucl. Mater.*, vol. 434, no. 1, pp. 141–151, 2013.

[18] T. Koyanagi, Y. Katoh, K. Ozawa, K. Shimoda, T. Hinoki, and L. L. Snead, "Neutron-irradiation creep of silicon carbide materials beyond the initial transient," *J. Nucl. Mater.*, vol. submitted, 2016.

[19] S. Kondo, T. Koyanagi, and T. Hinoki, "Irradiation creep of 3C–SiC and microstructural understanding of the underlying mechanisms," *J. Nucl. Mater.*, vol. 448, pp. 487–496, 2014.

[20] F. A. Garner, M. B. Toloczko, and B. H. Sencer, "Comparison of swelling and irradiation creep behavior of fcc-austenitic and bcc-ferritic/martensitic alloys at high neutron exposure," *J. Nucl. Mater.*, vol. 276, pp. 123–142, 2000.
[21] S. R. J. Saunders, H. E. Evans, M. Li, D. D. Gohil, and S. Osgerby, "Oxidation growth stresses in an alumina-forming ferritic steel measured by creep deflection," *Oxid. Met.*, vol. 48, no. 3–4, pp. 189–200, 1997.
[22] F. A. Garner and R. J. Puigh, "Irradiation creep and swelling of the fusion heats of PCA, HT9 and 9Cr-1Mo irradiated to high neutron fluence," *J. Nucl. Mater.*, vol. 179, pp. 577–580, 1991.
[23] M. M. Li, D. T. Hoelzer, M. L. Grossbeck, A. F. Rowcliffe, S. J. Zinkle, and R. J. Kurtz, "Irradiation creep of the US Heat 832665 of V-4Cr-4Ti," *J. Nucl. Mater.*, vol. 386–388, pp. 618–621, 2009.
[24] J. P. Foster and T. M. Karlsen, "Update of Irradiation Creep and Irradiation Stress Relaxation of 316 and 304L Stainless Steel, HWR-1047," OECD Halden Reactor Project, 2013.
[25] Y. Yamamoto, B. A. Pint, K. A. Terrani, K. G. Field, Y. Yang, and L. L. Snead, "Development and Property Evaluation of Nuclear Grade Wrought FeCrAl Fuel Cladding for Light Water Reactors," *J. Nucl. Mater.*, vol. 467, pp. 703–716, 2015.
[26] H. L. Heinisch, L. R. Greenwood, W. J. Weber, and R. E. Williford, "Displacement damage in silicon carbide irradiated in fission reactors," *J. Nucl. Mater.*, vol. 327, no. 2, pp. 175–181, 2004.
[27] A. Konobeyev, U. Fischer, and L. Zanini, "Advanced evaluations of displacement and gas production cross sections for chromium, iron, and nickel up to 3 GeV incident particle energy," in *Proceedings of the 10th International Topical Meeting on Nuclear Applications and Utilization of Accelerators, AccApp11. Knoxville, TN, US*, 2011.
[28] L. R. Greenwood and R. K. Smither, "SPECTER: Neutron Damage Calculations for Materials Irradiations, ANL/FPP/TM-197," Argonne National Laboratory, 1985.
[29] M. J. Norgett, M. T. Robinson, and I. M. Torrens, "A proposed method of calculating displacement dose rates," *Nucl. Eng. Des.*, vol. 33, pp. 50–54, 1975.
[30] SCDAP team, "SCDAP/RELAP5/MOD 3.2 Code Manual, Volume IV: MATPRO – A Library of Materials Properties for Light-Water-Reactor Accident Analysis," 1997.

Appendix A: Engineering Drawing of SiC Tensile Specimen for In-pile Creep Test

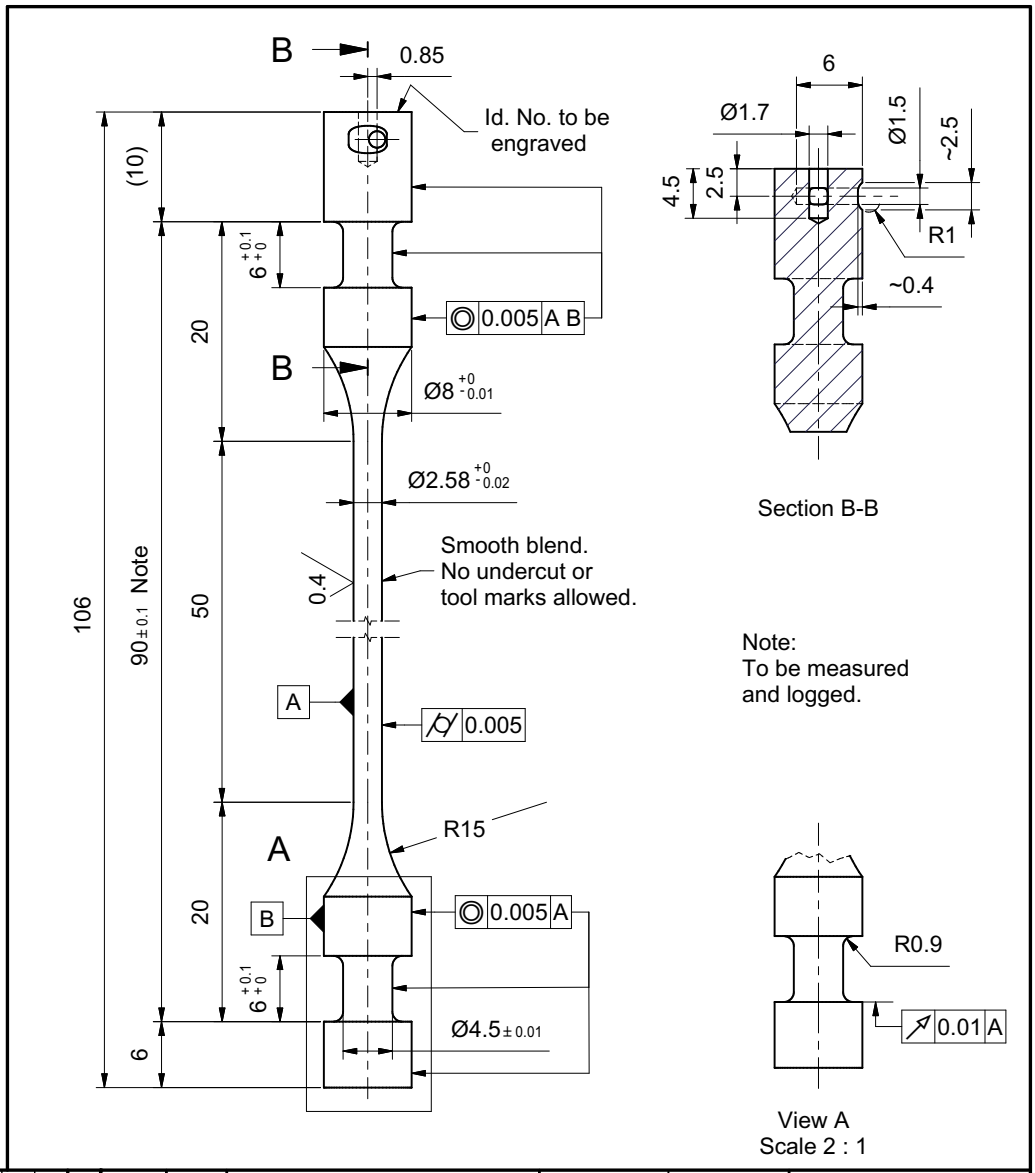

Qt.	Item	Description	Material	Dwg.no.	Remarks
		TOLERANCES UNLESS OTHERWISE SPECIFIED	General surface finish Ra um	0,8	REMOVE ALL BURRS AND SHARP EDGES

Nom.Size	Over		6	30	100	300	1000	ANGLES
Fit	To	6	30	100	300	1000	2000	
Fine	±	0,05	0,1	0,15	0,2	0,3	0,5	0,1°
Medium	±	0,1	0,2	0,3	0,5	0,8	1,2	0,25°
Coarse	±	0,2	0,5	0,8	1,2	2,0	3,0	1°

Correction	Date:	Project no.:	Designed:	Scale:	Institutt for energiteknikk
	07.02.2014	F-00132		2:1	OECD HALDEN REACTOR PROJECT
	Checked:		Approved:		HALDEN NORWAY

Date	Tensile Specimen SiC	Replacement for:	Replaced by:
	SiC Material in 744	491122	

Sign.	TSS no.:	Material: SiC	Art. no.

Appendix B: Engineering Drawing of FeCrAl Tensile Specimen for In-pile Creep Test